

## FLOW INTERACTIONS WITH BLUE MUSSEL PATCHES: HYDRODYNAMIC AND ECOLOGICAL IMPLICATIONS

ANDREW FOLKARD

*Lancaster Environment Centre, Lancaster University  
Lancaster, LA1 4YQ, United Kingdom*

TJEERD BOUMA

*Spatial Ecology Group, Royal Netherlands Institute for Sea Research (NIOZ),  
Korringaweg 7, 4401 NT Yerseke, the Netherlands*

In soft substrate inter-tidal and shallow sub-tidal environments, blue mussels (*Mytilus edulis*) form raised beds of enhanced surface roughness. These beds are rarely homogeneous and may be fractal in spatial structure, or organised into patches or stripes. In any case, the presence of multiple boundaries between regions occupied by mussels and regions of bare substrate are a common aspect of mussel beds. This spatial structure is thought to enable a balance to be achieved between the opposing controls of stress protection and food limitation. Both of these controls are governed strongly by the interaction of the mussels' spatial distribution with hydrodynamics, about which little is known. We address this knowledge gap. Specifically, we studied the effects of mussel patch density (mussels per unit area) and incident mean flow speed on the flow fields over and downstream of mussel patches via laboratory flume experiments. Velocity profiles were measured at several along-flume locations in each run, from which several hydrodynamic parameters were calculated. We found that mussel density is a strong determinant of flow structure over and downstream of mussel patches. As the incident flow passes over a patch, its vertical profile adjusts to the new, raised and roughened bed conditions. A second such adjustment occurs as the flow leaves the patch and re-finds the downstream bed. Turbulent energy is generated primarily at these adjustments to new bed conditions, and was enhanced by increased mussel density to a greater-than-linearly-proportional extent. This implies that there is advantage to higher density patches, in that they increase turbulent energy, enabling food to be mixed downwards to the mussels to an extent greater than the increased amount of mussels, so the amount of food per mussel increases.

### 1 INTRODUCTION

Blue mussels (*Mytilus edulis*) are sessile, benthic, bivalve filter feeders, and keystone species in many coastal environments. Their main food source, pelagic algae, is most commonly supplied by horizontal advection and vertical turbulent mixing [16]. Frechette et al. [10] found that the increased bed roughness due to the mussels enhances vertical turbulent transport, increasing the rate of supply of algae to themselves. Thus, via their physical structure, mussel beds increase vertical turbulent mixing and thereby vertical diffusion [2], drag coefficients [12] and patterns of particle deposition and resuspension [20]. This can significantly alter the structure and functioning of the whole coastal ecosystem in their landscape-scale vicinity [17]. As such, blue mussels play an important role in governing the diversity and spatial distribution of benthic macrofauna in soft-bottom habitats [5].

Mussels attach to hard surfaces to avoid being washed away by waves or tidal currents. In soft substrate environments, therefore, they cannot recruit directly to the bare substrate, but attach to hard objects lying on the bottom, especially each other's shells. As a result, mussels' spatial organisation in soft-bed environments is typically heterogeneous on multiple scales [11], and often has a striped or patchy structure with quasi-discontinuous edges [14]. This structure is thought to be due to a combination of competition for food and mutual facilitation by protecting each other against being washed away [19]. Since hydrodynamics provides both food supply and mechanical stresses to soft substrate mussel beds, their spatial distribution is predominantly a response to their interactions with the ambient hydrodynamics. Consequently, their functioning and resilience cannot be understood until these interactions, about which little is currently known, are understood. The novel contribution of the work reported here is to address this knowledge gap, by investigating the interactions of flows of water with isolated patches of mussels. We consider the effects of variations in both the speed of the flow and the density, and thus the height, of the patches of mussels.

## 2 METHODS

The experiment was carried out in the race-track flume at the Royal Netherlands Institute for Sea Research (NIOZ, Yerseke, the Netherlands), which is 17.55 m long and 600 mm wide [13], and was filled with seawater to a depth of 400mm throughout the experiment. Mussel patches were prepared using live mussels which were placed on boards whose width equalled that of the flume and were 1000mm in length. A standard mussel density (mussel density factor, MDF = 1) was first established by covering the board so that, as closely as possible, it was fully covered by a single layer of mussels, and counting the number of mussels. The density of mussels required to create this single layer coverage of the board –  $1008 \pm 9 \text{ m}^{-2}$  (mean  $\pm 1$  s.d;  $N = 5$ ) – was noted, and three further mussel densities were then established by halving (MDF = 0.5), doubling (MDF = 2) and tripling (MDF = 3) this density of mussels. These give mussel biomass per unit area values in the range 100–1452 g m<sup>-2</sup>, which correspond well with values provided in the literature [11]. At the start of each experimental run, one of these boards was secured in the test section of the flume, which was  $\approx 10$  m downstream of the start of one of the straight sections of the flume. During the measurements, there was negligible movement of mussels within or off the board. The experiment was then run by passing flow over the mussels at one of two mean flow speeds ( $U_0$ ), 20cms<sup>-1</sup> and 5cms<sup>-1</sup>. Measurements of the flow at numerous locations were then made with a Nortek Vectrino Acoustic Doppler Velocimeter (ADV, Nortek AS, Rud, Norway). We identify locations within the flume using along-flume (x), across flume (y) and vertical (z) coordinates, where  $x = 0$  is the location of the upstream end of the experimental mussel patch,  $y = 0$  is the central plane of the flume and  $z = 0$  is the location of the flume bed. Vertical profile measurements were made at 13 different heights at each of 10 downstream locations:  $x = -100$ mm (i.e. 100mm upstream of the patch),  $x = 300, 600$  and  $900$ mm (over the patch) and  $x = 1100, 1400, 1700, 2000, 2400$  and  $2800$ mm (downstream of the patch). For each x-z location, measurements were made at three across-flume (y) positions. In addition, each treatment (combination of MDF and  $U_0$  values) was tested in three runs, using a different replicate of the mussel patch each time. Thus, nine replicates measurements were at each x-z location for each treatment.

Components of mean flow speed in the along-flume (u), across-flume (v) and vertical (w) directions were calculated from each time series of three-dimensional ADV velocity measurements {U(t),V(t),W(t)} for each location. These mean speeds were then subtracted from the corresponding initial time series to give time series of fluctuating velocity components U'(t), V'(t) and W'(t) (i.e. U'(t) = U(t)-u etc.). Turbulent flow components u', v' and w' were calculated as the root mean square values of these fluctuating component time series. The along-flume:vertical component of Reynolds stress was calculated as

$$Re_{uw} = -\rho \overline{U'(t)W'(t)} \quad (1)$$

where  $\rho$  is the density of the seawater used (1028kgm<sup>-3</sup>), and other Reynolds stress components (e.g.  $Re_{vw}$ , used below in the bed shear stress calculation) were calculated in the same way. The turbulent kinetic energy per unit mass of water at each measurement point was calculated as

$$TKE = \frac{1}{2} (u'^2 + v'^2 + w'^2) \quad (2)$$

Finally, bed shear stress was calculated as

$$\tau_0 = \left\{ \mu \frac{\partial u}{\partial z} + (Re_{uw}^2 + Re_{vw}^2)^{1/2} \right\}_{z=0} \quad (3)$$

where  $\mu = 10^{-3}$  kgm<sup>-1</sup>s<sup>-1</sup> is the dynamic viscosity of water, the terms on the right hand side due to mean flow ( $\mu \partial u / \partial z$ ) and turbulence ( $Re_{uw} + Re_{vw}$ ) also being considered individually. Comparisons between  $\mu \partial u / \partial z$  and  $\mu u^2$ , an alternative expression for the mean flow bed shear stress, showed them to be approximately equivalent.

### 3 RESULTS

#### 3.1 Mean flow profiles

The range of measured flow patterns is illustrated (Figure 1) by comparing the vertical profiles of  $u/U_0$  for the two extreme cases of the  $U_0$  and MDF values used, ( $U_0 = 20 \text{ cms}^{-1}$ , MDF = 3) and ( $U_0 = 5 \text{ cms}^{-1}$ , MDF = 0.5). The flow scales linearly with the mean incident flow speed. There are, however, clear differences between the profiles for different MDF values due to differences in the height of the patches and, possibly, their roughness. These result in greater vertical velocity gradients in the MDF = 3 profiles than in the MDF = 0.5 profiles.

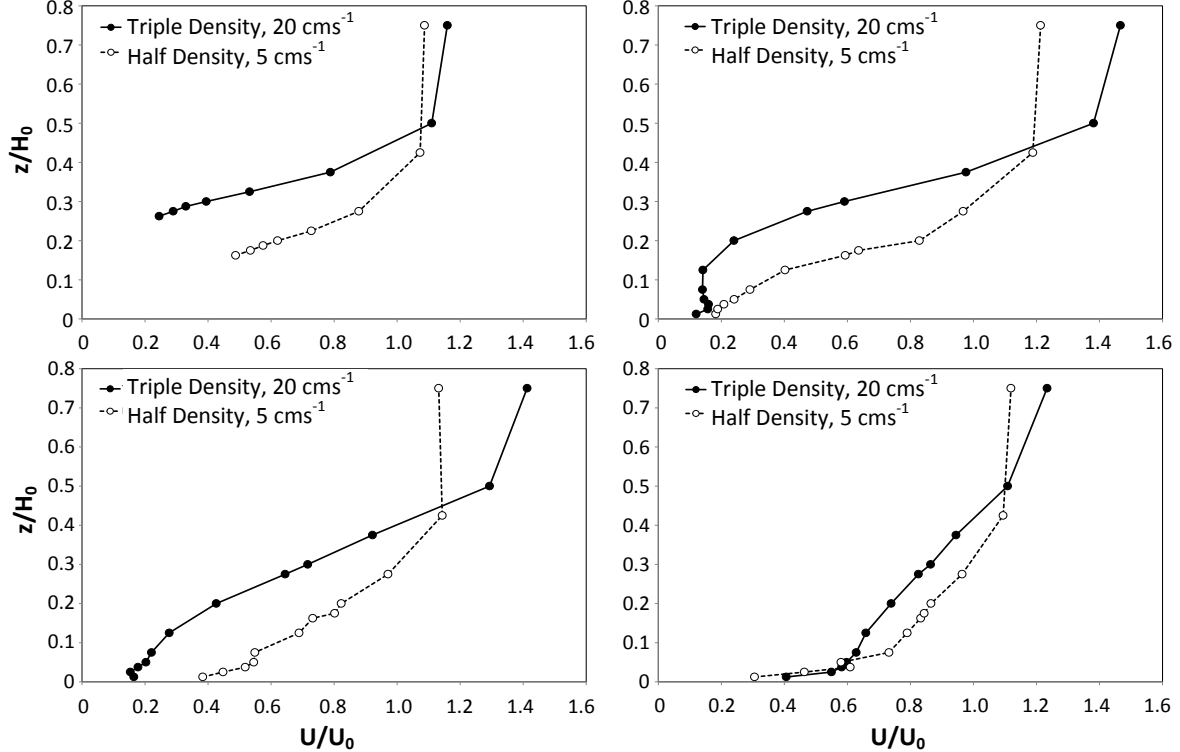


Figure 1: Vertical profiles of downstream flow speed ( $u$ ) normalised by mean flow speed ( $U_0$ ) for the cases ( $U_0 = 20 \text{ cms}^{-1}$ , MDF = 3) and ( $U_0 = 5 \text{ cms}^{-1}$ , MDF = 0.5), at downstream locations  $x = 900\text{mm}$  (top left),  $1100\text{mm}$  (top right),  $1700\text{mm}$  (middle left),  $2800\text{mm}$  (middle right) and  $2800\text{mm}$  (bottom).  $H_0$  is flow depth (400mm)

#### 3.2 Turbulence profiles

In established boundary layers, turbulent velocity scales are assumed to scale with the shear velocity, since the turbulence is generated by the shear. Thus, turbulent kinetic energy (TKE) is usually normalised by  $u^*{}^2$ . Here, however, the definition of  $u^*$  is complicated – the boundary layers are evolving rather than established, and there are two shear layers – one created by the mussel patch and the other by the flume bed. Thus, normalising by  $u^*{}^2$  was not helpful here and instead we normalised by the mean flow kinetic energy per unit volume,  $\frac{1}{2}\rho U_0^2$ .

The general pattern of evolution of TKE (Figure 2) is that, starting from low upstream levels ( $x = -100\text{mm}$ ), flow over the patch creates a turbulence maximum close to the mussels ( $x = 900 \text{ mm}$ ), but this is exceeded by the bloom of turbulent energy created immediately downstream of the patch, and the shear here – between the flow that has passed over the patch and the fluid beneath it in the lee of the patch – creates the global turbulence maximum ( $x = 1100\text{mm}$  and  $1700\text{mm}$ ), which then spreads vertically and decays downstream ( $x = 2800\text{mm}$ ). There are notable differences between the two extreme cases shown in Figure 2: in the ( $U_0 = 20 \text{ cms}^{-1}$ , MDF = 3) case, the turbulence bloom is relatively wide (vertically) and doesn't peak until  $x = 1700\text{mm}$ , decaying strongly thereafter as the mean flow shear decreases. In the ( $U_0 = 5 \text{ cms}^{-1}$ , MDF = 0.5) case, the turbulence bloom is relatively narrow and peaks sooner ( $x = 1100\text{mm}$ ).

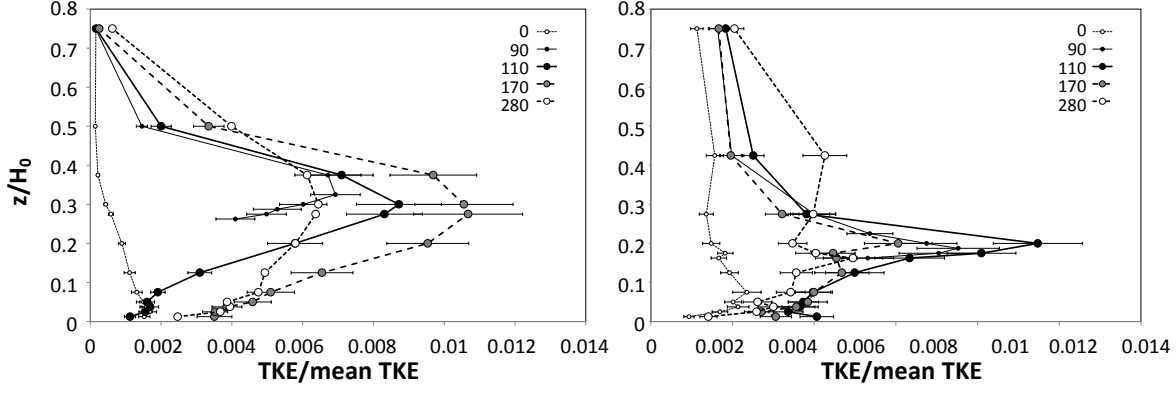


Figure 2: Downstream evolution of the vertical profile of turbulent kinetic energy (TKE) normalised by mean flow kinetic energy ( $\frac{1}{2}\rho U_0^2$ ) for ( $U_0 = 20 \text{ cm s}^{-1}$ , MDF = 3) (left) and ( $U_0 = 5 \text{ cm s}^{-1}$ , MDF = 0.5) (right)

These differences can also be seen in the downstream evolution of the depth integrated turbulent kinetic energy (Figure 3). In all of the  $U_0 = 20 \text{ cm s}^{-1}$  cases, there is a clear pattern of a rise to a peak at  $x = 1400\text{--}1700 \text{ mm}$ , and a monotonic decay thereafter. In the  $U_0 = 5 \text{ cm s}^{-1}$  cases, there is a peak at  $x = 1100 \text{ mm}$ , then only a weak decay. The peak depth-integrated TKE scales well with the mean flow kinetic energy  $\frac{1}{2}\rho U_0^2$ , as do the peak values of the Reynolds stress component  $Re_{uw}$  (Figure 4). There is also a consistent variation of these parameters with mussel patch density: given the limited range of MDF values tested here, there are various curves that could fit the portion of this variation shown in Figure 4, but the values appear to be approximately constant for  $MDF \leq 1$  and to increase non-linearly in the range  $1 < MDF < 3$ .

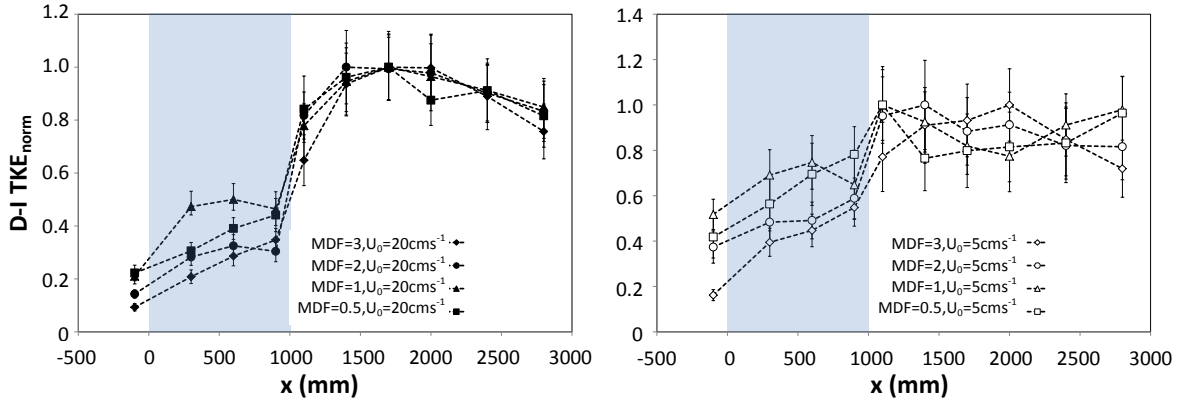


Figure 3: Downstream evolution of the depth-integrated turbulent kinetic energy, normalised by its maximum value in each run, for  $U_0 = 20 \text{ cm s}^{-1}$  cases (left) and  $U_0 = 5 \text{ cm s}^{-1}$  cases (right). The shaded region indicates the along-flume location of the mussel patch

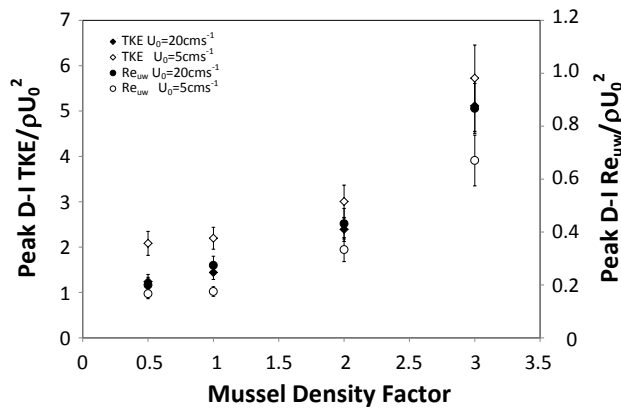


Figure 4: Variation of the peak values of depth-integrated turbulent kinetic energy and Reynolds stress component with mean flow speed ( $U_0$ ) and mussel patch density factor (MDF)

### 3.3 Bed shear stress

The bed shear stress varies with both  $U_0$  and MDF (Figure 5). In all cases, there is a minimum immediately downstream of the patch, where the bed is sheltered by the patch. Thereafter, the turbulent stress peaks shortly downstream of the patch, then decays away, while the mean flow stress becomes increasingly dominant downstream. By the end of the measurement field, the mean flow stress is several times larger than turbulent shear stress, as would be expected in stable boundary layers.

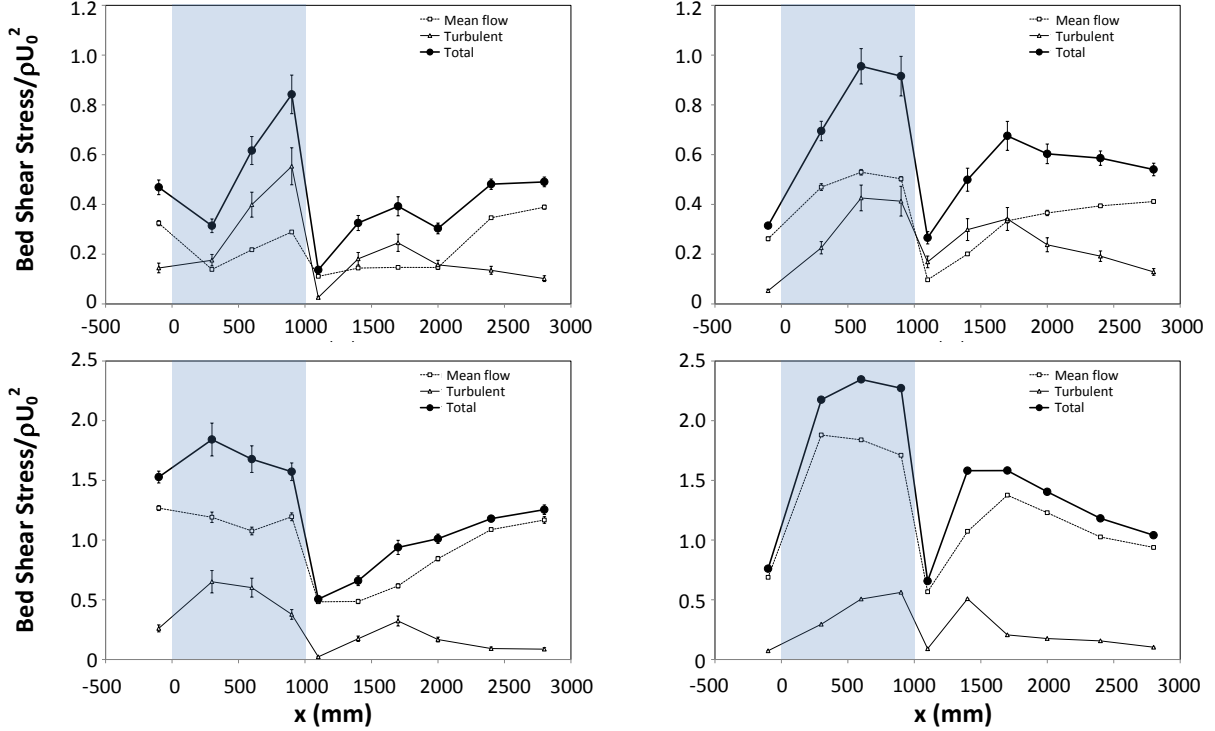


Figure 5: Downstream evolution of bed shear stress for  $U_0 = 20\text{cm s}^{-1}$  cases (top) and the  $U_0 = 5\text{cm s}^{-1}$  cases (bottom) with MDF = 3 (left) and MDF = 0.5 (right). The shaded region indicates the along-flume location of the mussel patch

## 4 DISCUSSION

Wake structures behind patches of aquatic organisms remain surprisingly poorly studied (but see [8,9,21]), despite their importance for ecological functioning, especially in patchy environments. The wake structure observed in these experiments is similar to that reported by Folkard [7] downstream of seagrass patches, in that there is a “near wake” region in which TKE and Reynolds stresses increase immediately downstream of the patch, before decaying in the “far wake” and eventually (presumably) returning to their upstream state, in equilibrium with the smooth flume bed (Figure 3). It also provides further evidence to support the finding of [9] that mussel patch edges, and in particular their downstream edges, are the primary sites of turbulence production when flows pass over spatially-patterned mussel beds (Figure 3).

The “bloom” of turbulence at the downstream edge of the patch (Figure 2) is caused by the shear between the flow that has passed over the patch and the stagnant flow beneath it, which is sheltered by the mussel patch. As this shear decays, so does the turbulent energy and the “far-wake” begins. In fluid dynamical terms, therefore, the mussel patch is an intermediate form of roughness structure, between changes in bed roughness that do not coincide with changes in bed height, such as transitions from open water to ice on lakes, or grassland to bare soil [3,4] and vertically-extended canopies such as forests and urban buildings [1,15]. This suggests that a detailed model of the dynamics of the flow over mussel patches, of the sort provided by for example [1] for the latter type of canopy, would provide valuable insights into how mussels interact with their physical environment.

The structure of flow over patterned mussel beds is controlled by a number of characteristics of the mussel bed configuration. Folkard & Gascoigne [9] showed that the density of patch edges is one such characteristic. The

findings of [8], although they refer canopies of aquatic vegetation, suggest that patch separation is also important. Folkard & Gascoigne [9], along with unpublished data (D. McGovern, pers. comm.), suggest that mussel patches wipe any memory of upstream conditions from the flow and turbulence profiles within distances of less than 1 m. In contrast, the “memory” of a mussel patch in the flow profile (i.e. the altered flow structure in the patch’s wake, and the associated enhanced bed shear stress) is retained a long way downstream of the patch if the flow subsequently passes over a smooth bed. These experiments did not have long enough measurement sections to capture the full extent of these wakes, but a study of airflow over lakes downstream of forest canopies [15] suggests that they extend for the order of 50 canopy heights (3-5m in the case of the present experiment). This asymmetry, between the mussel patches rapidly wiping the memory of upstream structure from the flow profile, and flow profiles’ long memory of upstream mussel patches, demonstrates the mussels’ strong ecosystem engineering effect on their environment. Here, we have shown that mussel patch height is a dominant parameter in governing the way in which this coupling occurs.

Differences in the magnitude of flow parameters due to incident flow speed were generally found to be proportional to  $U_0$  (Figure 1), or  $U_0^2$  for parameters which have a quadratic relationship with flow velocity, such as the depth integrated TKE (Figure 4). The main discrepancy was TKE downstream of the patch (Figure 3). In the more energetic runs, the turbulence bloom was strong and vertically extended. In the weaker runs, it was weak and vertically constrained. Changes in flow structure due to variations in mussel patch density had more variety. In the patch wake, the most important density effect is that the ratio of peak TKE to MDF increases with increasing MDF (Figure 4). Preliminary experiments showed that the same amount of mussels spread out over a larger area don’t have the same effect. Thus there is a value to having higher density patches of mussels in that it enables food to be mixed downwards to an extent greater than the increased amount of mussels, so the amount of food per mussel increases. Clearly, there are trade-offs. As the density of mussels increases, mussels at the bottom of the pile will become unable to access the food. Thus, the benefits are more closely associated with changes – particularly sudden ones – in bed height, rather than mussel density *per se*. Therefore, the tendency in nature for mussels to sit atop mounds of sediment, empty shells and other detritus [5] and distributed in fragment patterns with multiple edges, rather than homogeneously [14] is consistent with this finding.

The TKE increases more at the patch edges than over the patch itself. The implications of this density-enhanced mixing on food supply modelling [18] can be considered. If the rate of food supply due to vertical turbulent mixing over a patch is equal to or greater than the optimum uptake rate of the mussels, then there is enough food for all mussels and no limit to patch size imposed by food supply. However, in cases, where the optimum uptake rate of the mussels is greater than the rate of vertically-mixed food supply, there will be a region at the front of the patch where food is available via horizontal advection from upstream, but downstream of this there will be insufficient food. As a result, patches will be limited in length to the extent of the advectively-supplied region, and widely enough spaced to allow replenishment between patches. This is the conceptual picture put forward by [18]. The present study adds that increasing the mussel density in patches by a factor  $M$  increases the rate of replenishment by vertical mixing by a factor greater than  $M$ . In vertical food supply-limited cases, this will allow smaller gaps between patches and thus an overall increase in mussel density. Thus there is an advantage to increased mussel density in patches due to their hydrodynamic effects under these conditions.

## 5 CONCLUSIONS

We carried out laboratory flume experiments using patches of live mussels, varying incident mean flow speed and the density of mussels within the patches, and therefore the height above the bed of the patches. We performed measurements of vertical profiles of hydrodynamic parameters at locations upstream, over and downstream of the patches. From analysis of these measurements, we conclude:

- Mussel bed height was a dominant parameter in determining the structure of the flow over and downstream of mussel patches. As the incident flow passed over a mussel patch, it adjusted to the new bed conditions the patch presented. Downstream of the patch, the profile retained a memory of the effects of the patch as far as (and presumably beyond) the end of the experimental section of the flume.
- Turbulence was generated primarily where the flow adjusted to new boundary conditions. It peaked shortly downstream of the patch, the wake structure being similar to that reported by [7] in that there was a “near wake” region where turbulent energy increased downstream, followed by a “far wake” in which it decreased. Depth integrated TKE scaled with  $U_0^2$  and was enhanced by increased mussel bed

height to a greater-than-linearly-proportional extent. This implies that there is an advantage to mussels congregating in higher patches, in that it increases the TKE, which enables food to be mixed downwards to an extent greater than the increased amount of mussels, so the amount of food per mussel increases. In all cases, bed shear stress had a minimum in the sheltered region immediately downstream of the patch, whereafter it increased, peaked and died away as the flow profile returned to equilibrium with the bare flume bed, a process which took longer in the higher patch cases.

## REFERENCES

- [1] Belcher S., Jerram N. and Hunt J. "Adjustment of a turbulent boundary layer to a canopy of roughness elements", *Journal of Fluid Mechanics*, Vol. 488 (2003) pp 369-398.
- [2] Butman C., Frechette M., Geyer R. and Starczak V. "Flume experiments on food supply to the blue mussel *Mytilus edulis* L. as a function of boundary-layer flow", *Limnology and Oceanography*, Vol. 39, No. 7 (1994) pp 1755-1768.
- [3] Chamorro L. and Porté-Agel F. "Velocity and surface shear stress distributions behind a rough-to-smooth surface transition: a simple new model", *Boundary Layer Meteorology* Vol. 130 (2009) pp 29-41.
- [4] Chen X.W. and Chiew Y.-M. "Response of velocity and turbulence to sudden change of bed roughness in open-channel flow", *Journal of Hydraulic Engineering (ASCE)* Vol. 129 (2003) pp 35-43.
- [5] Commito J., Celano E., Celico H., Como S. and Johnson C. "Mussels matter: postlarval dispersal dynamics dynamics altered by a spatially complex ecosystem engineer", *Journal of Experimental Marine Biology and Ecology* Vol. 316 (2005) pp 133-147.
- [6] Commito J., Dow W. and Grupe B. "Hierarchical structure in soft-bottom mussel beds", *Journal of Experimental Marine Biology and Ecology* Vol. 330 (2006) pp 27-37.
- [7] Folkard A. "Hydrodynamics of model *Posidonia oceanica* patches in shallow water", *Limnology and Oceanography* Vol. 50 (2005) pp 1592-1600.
- [8] Folkard A. "Flow regimes in gaps within stands of flexible vegetation: laboratory flume simulations", *Environmental Fluid Mechanics* Vol. 11 (2011) pp 289-306.
- [9] Folkard A. and Gascoigne J. "Hydrodynamics of discontinuous mussel beds: laboratory flume simulations", *Journal of Sea Research* Vol. 62 (2009) pp 250-257.
- [10] Frechette M., Butman C. and Geyer R. "The importance of boundary-layer flows in supplying phytoplankton to the benthic suspension feeder, *Mytilus edulis* L.", *Limnology and Oceanography* Vol. 34 (1989) pp 19-36.
- [11] Gascoigne J., Beadman H., Saurel C. and Kaiser M. "Density dependence, spatial scale and patterning in sessile biota", *Oecologia* Vol. 145 (2005) pp 371-381.
- [12] Green M., Hewitt J. and Thrush S. "Seabed drag coefficient over natural beds of horse mussels (*Atrina zelandica*)", *Journal of Marine Research*, Vol. 56, No. 3, (1998) pp 613-637.
- [13] Jonsson P., van Duren L., Amielh M., Asmus R., et al. "Making water flow: a comparison of the hydrodynamic characteristics of 12 different benthic biological flumes", *Aquatic Ecology*, Vol. 40, No. 4 (2006) pp 409-438.
- [14] Liu Q.-X., Herman P., Mooij W., Huisman J., Scheffer M., Olff H. and van de Koppel, J., "Pattern formation at multiple spatial scales drives the resilience of mussel bed ecosystems", *Nature Communications*, Vol. 5 (2014) doi: 10.1038/ncomms6234.
- [15] Markfort C., Perez A., Thill J., Jaster D., Porté-Agel F. and Stefan H. "Wind sheltering of a lake by a tree canopy or bluff topography", *Water Resources Research*, Vol. 46 (2010) Article Number W03530.
- [16] Simpson J., Berx B., Gascoigne J. and Saurel C. "The interaction of tidal advection, diffusion and mussel filtration in a tidal channel", *Journal of Marine Systems*, Vol. 68 (2007) pp 556-568.
- [17] Sousa R., Gutiérrez J. and Aldridge D. "Non-indigenous invasive bivalves as ecosystem engineers", *Biological Invasions*, Vol. 11, No. 10 (2009) pp 2367-2385.
- [18] van de Koppel J., Rietkerk M., Dankers N. and Herman P. "Scale-dependent feedback and regular spatial patterns in young mussel beds", *American Naturalist*, Vol. 165 (2005) pp E66-E77.
- [19] van de Koppel J., Gascoigne J., Theraulax G., Rietkerk M., Mooij W. and Herman P. "Experimental evidence for spatial self-organisation and its emergent effects in mussel bed ecosystems", *Science*, Vol. 322 (2008) pp 739-742.
- [20] van Leeuwen B., Augustijn D., van Wesenbeeck B., Hulscher S. and de Vries M. "Modeling the influence of a young mussel bed on fine sediment dynamics on an intertidal flat in the Wadden Sea", *Ecological Engineering*, Vol. 36, No. 2 (2010) pp 145-153.

[21] Zong L. and Nepf H. "Vortex development behind a finite porous obstruction in a channel", *Journal of Fluid Mechanics*, Vol. 691 (2012) pp 368-391.